



ORIGINAL ARTICLE

High prevalence of deleterious mutations in concomitant nonsyndromic cleft and outflow tract heart defects

Naikhoba C. O. Munabi¹  | Shady Mikhail² | Omar Toubat³ | Michelle Webb⁴ | Allyn Auslander² | Pedro A. Sanchez-Lara⁵ | Zarko Manojlovic⁴ | Ryan J. Schmidt^{6,7} | David Craig⁴ | William P. Magee III^{1,8,9} | Subramanyan Ram Kumar^{3,10} 

¹Division of Plastic and Reconstructive Surgery, Keck School of Medicine of USC, Los Angeles, California, USA

²Operation Smile Inc, Virginia Beach, Virginia, USA

³Division of Cardiac Surgery, Department of Surgery, Keck School of Medicine of USC, Los Angeles, California, USA

⁴Department of Translational Genomics, Keck School of Medicine of USC, Los Angeles, California, USA

⁵Department of Pediatrics, Cedars-Sinai Medical Center, Los Angeles, California, USA

⁶Department of Pathology and Laboratory Medicine, Children's Hospital Los Angeles, Los Angeles, California, USA

⁷Department of Pathology, Keck School of Medicine of USC, Los Angeles, California, USA

⁸Division of Plastic and Maxillofacial Surgery, Children's Hospital Los Angeles, Los Angeles, California, USA

⁹Department of Plastic Surgery, Shriners Hospital for Children, Los Angeles, California, USA

¹⁰Heart Institute, Children's Hospital Los Angeles, Los Angeles, California, USA

Correspondence

Subramanyan Ram Kumar, Division of Cardiac Surgery, Children's Hospital Los Angeles, 4650 Sunset Boulevard, Mailstop #66, Los Angeles, CA 90033, USA.
Email: rsubramanyan@surgery.usc.edu

Funding information

National Center for Advancing Translational Sciences, Grant/Award Number: UL1TR000242

Abstract

Our previous work demonstrating enrichment of outflow tract (OFT) congenital heart disease (CHD) in children with cleft lip and/or palate (CL/P) suggests derangements in common underlying developmental pathways. The current pilot study examines the underlying genetics of concomitant nonsyndromic CL/P and OFT CHD phenotype. Of 575 patients who underwent CL/P surgery at Children's Hospital Los Angeles, seven with OFT CHD, negative chromosomal microarray analysis, and no recognizable syndromic association were recruited with their parents (as available). Whole genome sequencing of blood samples paired with whole-blood-based RNA sequencing for probands was performed. A pathogenic or potentially pathogenic variant was identified in 6/7 (85.7%) probands. A total of seven candidate genes were mutated (*CHD7*, *SMARCA4*, *MED12*, *APOB*, *RNF213*, *SETX*, and *JAG1*). Gene ontology analysis of variants predicted involvement in binding (100%), regulation of transcription (42.9%), and helicase activity (42.9%). Four patients (57.1%) expressed gene variants (*CHD7*, *SMARCA4*, *MED12*, and *RNF213*) previously involved in the Wnt signaling pathway. Our pilot analysis of a small cohort of patients with combined CL/P and OFT CHD phenotype suggests a potentially significant prevalence of deleterious mutations. In our cohort, an overrepresentation of mutations in molecules associated with Wnt-signaling was found. These variants may represent an expanded phenotypic heterogeneity within known monogenic disease genes or provide novel evidence of shared developmental pathways. The mechanistic implications of these mutations and subsequent developmental derangements resulting in the CL/P and OFT CHD phenotype require further analysis in a larger cohort of patients.

KEYWORDS

cleft lip, cleft palate, congenital heart disease, genetic syndrome, whole genome sequencing

This is an open access article under the terms of the [Creative Commons Attribution-NonCommercial-NoDerivs](https://creativecommons.org/licenses/by-nc-nd/4.0/) License, which permits use and distribution in any medium, provided the original work is properly cited, the use is non-commercial and no modifications or adaptations are made.

© 2022 The Authors. *American Journal of Medical Genetics Part A* published by Wiley Periodicals LLC.

1 | INTRODUCTION

Congenital birth defects occur in ~3% of all births and are the leading cause of death among infants in the United States (Centers for Disease Control and Prevention, 2019; Heron, 2016). In addition to the mortality burden, birth defects are also a significant source of hospital resource utilization and health care expenditure (Arth et al., 2017). Not infrequently, developmental defects in multiple organ systems tend to coexist in the same individual. In some clinical conditions, such as VACTERL, the patient may harbor specific morphologic features that are developmentally unrelated, yet nonrandomly associated (van de Putte et al., 2020). Alternatively, in other cases, concomitant lesion sets may derive from a common genetic or molecular event, such as 22q11.2 deletions in DiGeorge syndrome or Fibrillin-1 gene mutations in Marfan syndrome (Grygiel-Gorniak et al., 2020; Lackey & Muzio, 2021). Understanding the developmental events that result in coexisting birth defects is not only important for accurately determining the underlying mechanisms of disease but may also improve prognostic and therapeutic efforts.

Children's Hospital Los Angeles is a tertiary referral center that has established expertise in caring for pediatric craniofacial and cardiac disorders. This clinical experience has enabled identification of patients with combined cleft and cardiac malformations as a niche cohort in which to study concomitant birth defects. Cleft lip and/or palate (CL/P) is the most common congenital birth defect of the head and neck, with an incidence of 1 in 700 live births (Mossey & Catilla, 2001; Mossey & Modell, 2012; Munabi et al., 2017). Approximately 70% of patients with CL/P patients have no recognizable syndrome (Mossey & Catilla, 2001; Mossey & Modell, 2012; Munabi et al., 2017). Nevertheless, patients with CL/P have considerably higher rates of coexisting congenital anomalies compared to the general population, with incidences varying from 14% to 66% across studies and populations (Munabi et al., 2017). Congenital heart disease (CHD) is the most common congenital birth defect worldwide with an incidence of 8–12 per 1000 live birth (Heron, 2016; Mossey & Catilla, 2001; Mossey & Modell, 2012). Within CL/P patients, CHD accounts for more than a third of all associated anomalies (Mossey & Catilla, 2001; Mossey & Modell, 2012; Munabi et al., 2017).

While previous reports have described the relationship between cleft and cardiac defects in the context of specific genetic syndromes, our work has shown that this relationship persists in nonsyndromic CL/P (nsCL/P) patients as well. In particular, we found that nsCL/P patients experienced a 14-fold greater birth prevalence of CHD than observed in the general population (Azadgoli et al., 2020), with an enrichment of outflow tract (OFT) heart defects (Toubat et al., 2021). We also demonstrated that the co-existence of these lesions adversely impacts the surgical management of both cleft and cardiac defects (Azadgoli et al., 2020; Toubat et al., 2021). A 2017 study using next generation sequencing identified a mutation in the MTHFR gene, which was likely the pathogenic variant resulting in CHD and cleft in a single patient (Liu et al., 2017). Aside from this study and despite the highly clinically relevant association, the molecular and genetic basis of combined CHD and nsCL/P is largely unknown.

We hypothesized that concomitant nsCL/P and OFT CHD likely results from a shared molecular etiology. This study aims to identify underlying genetic abnormalities in a pilot cohort of patients with nsCL/P and OFT CHD, using whole genome sequencing paired with whole-blood-based RNA sequencing (RNA-seq).

2 | METHODS

2.1 | Editorial policies and ethical consideration

The study was approved by the institutional review boards of Children's Hospital Los Angeles and the University of Southern California. Written consent was obtained from all available parents of study participants.

2.2 | Patient selection

Retrospective review of 575 patients who underwent surgery for CL/P at CHLA over a 9-year period was performed. Eighty-three patients (14.4%) were found to have a concomitant diagnosis of CHD. Patients underwent further review by a multidisciplinary team including a medical geneticist, cardiothoracic surgeon, plastic surgeon, and craniofacial biologist. Twenty patients had prior genetic testing with negative chromosomal microarray analysis and were eligible for study inclusion. Patients with a known genetic mutation from diagnostic testing at an outside institution were excluded leaving 13 patients (65%) who were contacted for study participation.

Study design was an analysis of patient cases and unaffected biologic parents who were available for participation. Seven patients with nsCL/P agreed to participate and was consented for study participation. Four patients presented as complete trios with both parents, three with one parent only as duos. One of the trio patients presented with triplet siblings who were also included as a family study. Patients underwent a facial and clinical cardiac exam and questionnaire interview. Whole blood samples were collected for DNA and RNA extraction from patients and DNA extraction only from parents. RNA analysis was only performed for trios who did not have a pathogenic variant identified on DNA analysis.

2.3 | Nucleic acid extractions and analysis

Whole blood was collected in PAXgene Blood DNA or RNA Tubes (Biosciences, La Jolla, CA) and DNA or RNA was extracted using either PAXgene Blood DNA or RNA Kits (Qiagen, Venlo, Netherlands). Both DNA and RNA were assessed using the NanoDrop (Thermo Scientific, Waltham, MA), Qubit (Invitrogen, Carlsbad, CA), and TapeStation (Agilent Technologies, Santa Clara, CA). Nucleic acids had quality of DIN score > 7.5 and RIN > 6.

For whole genome sequencing, 500 ng of DNA greater than 200 bp was sheared in 130 μ l of nuclease-free water with the Covaris

E220 using the 96 microTUBE Plate (Covaris, Woburn, MA). DNA was quantified using the High Sensitivity D1000 Screen Tape Assay (Agilent Technologies, Santa Clara, CA). DNA libraries were prepared with the KAPA Hyper Prep Kit (Roche, Basel, Switzerland). Dual-indexed adapters were ligated to end-prepped and a-tailed DNA. The prepared libraries were quantified using D1000 Screen Tape Assay (Agilent Technologies, Santa Clara, CA). For RNA-seq, 200 ng were heat fragmented to a target size of 180 bp. Fragmented molecules were used for library prep using the NEBNext® Ultra™ II Directional RNA Library Prep Kit for Illumina (New England BioLabs, Inc., Ipswich, MA) and NEBNext Poly(A) mRNA magnetic isolation module.

Each library was normalized to 5 nM, pooled, and sequenced on NovaSeq 6000, using the NovaSeq S4 300 cycles flow cell V1 chemistry (Illumina, San Diego, CA). All sequencing reads were converted using BCL2FASTQ v2.19.1.403 to generate industry standard FASTQs. High resolution whole genome sequencing generated 207,681 Mb of data on average, 62.9× estimated depth of coverage, and 95.1% of data above 20×. An average of 107.1 million uniquely mapped RNA reads were generated of which 87.1% were assigned to mRNAs.

2.4 | Data analysis

DNA sample FASTQs were aligned to GRCh37 (hs37d5) using BWA-MEM (v0.7.8; Li, 2013). Post-processing included base recalibration, duplicate read marking, and joint indel realignment using GATK (v3.5.0). Germline variants and indels were obtained using GATK Haplotype Caller, Samtools (v1.2) mpileup paired with BCFtools (v1.2). VCFs were annotated with SnpEff (v3.5h), using a dbSNP (v137.b37) reference (DePristo et al., 2011). Copy number analysis was completed using tCoNuT (Aldrich, 2020).

RNA sample FASTQs were aligned to GRCh37 (hs37d5) using STAR (v2.5.3a) (Dobin et al., 2013). Post-processing included duplicate marking and splitting of N cigar reads with GATK Transcript

quantification using Salmon (v0.7.2) with a GRCh37.74 hs37d5 GTF reference. Cufflinks (v2.2.1) was used for isoform quantification (Trapnell et al., 2010). Sample alignment metrics for both DNA and RNA were obtained using Picard Tools v(1.128) and Samtools stats. In addition, Picard Tools GC coverage bias and hybrid-selection metrics were obtained for DNA.

Prioritization was given to functionally impactful variants following a known Mendelian disease model. Briefly, to identify high confidence variants for study, SnpEff annotated Haplotype Caller VCFs were filtered for read quality, read depth, variant functional effect, modes of inheritance across trios, and prevalence in population databases. Variants found in <1% of the 1000 Genomes phase 3 or gnomAD (version 2) populations or within the gnomAD were defined as rare. Variants with a quality score above 500 were investigated for significance and pathogenicity leveraging dbNSFP (version 3.2) and Clinvar databases (04/2016; Landrum et al., 2018; Liu et al., 2016). Protein ANalysis THrough Evolutionary Relationships (PANTHER) classification system (<http://www.pantherdb.org/>), the Database for Annotation, Visualization, and Integrated Discovery (DAVID) software (<https://david.ncifcrf.gov/home.jsp>), and a primary literature review were used to evaluate gene function, gene ontology, and associated pathways for each candidate gene. For molecular function and biological processes, only the top five associated categories across variants were listed.

2.5 | Variant filtering approach

To identify high confidence variants for study, the original HaplotypeCaller vcf files were annotated with a custom automated tool that leverages dbNSFP (version 3.2), Clinvar databases, PANTHER classification system, and the DAVID software. Annotations for variants discussed in the article are in Table 1. The resultant files were exported as excel files and manually evaluated through the following process. First, variants were filtered for quality scores >300 and

TABLE 1 Variant quality, pLI, and CADD Phred score for each isolated variant

Proband	Gene	Position	rsID	Effect	Quality	pLI	CADD_phred	ACMG/AMP criteria
1	CHD7	chr8:61736576	None	Splicing Acceptor/ Donor Loss	488	1.0	27	Pathogenic (PVS1, PS2, PM2)
2	SMARCA4	chr19:11134270	rs797045981	R979Q	1046	1.0	35	Pathogenic (PS2, PM2 moderate, PS4, PP3, PP5)
3	MED12	chrX:70349038	None	Q1184fs	658	1.0	None	Pathogenic (PVS1, PS2, PM2)
4	APOB	chr2:21225528	rs61743313	E4256K	2231	0	4.3	VUS (BP4)
4	APOB	chr2:21228483	rs61741974	F3753L	2962	0	22	VUS (BP4)
(Duo) A	RNF213	chr17:78280054	None	S738N	1361	0.0	0.1	VUS (BP4)
(Duo) A	SETX	chr9:135140170	rs61735488	S2497N	1225	0.2	15	VUS (BP4)
(Duo) A	SETX	chr9:135205642	rs370363342	D448G	2068	0.2	22	VUS (BP4)
(Duo) B	JAG1	chr20:10620243	rs755420729	N1187S	832	1.0	0.2	VUS (BP4)

sorted in descending order. Depending on the results, an increased filter of 500 was applied for some samples. Variants with missing information or multiallelic entries in the genotype columns across the sets were removed. Genes with <5 novel occurrences in gnomAD were kept for further analysis. Next, varied modes of inheritance across the samples were tested in an iterative approach. For example, de novo variants in probands with trio information were identified by searching for variants present in the proband but not in the parent samples. For the duo samples, identification of variants in this step was done with more flexibility, as not enough information was present to make definite determination on inheritance for the proband.

For each iterative process, allelic depth was the next consideration. A hard filter was not applied to remove variants, but generally, only variants with coverage above 10 reads per allele were accepted for further inquiry. Functional effect, probability of being loss-of-function intolerant (pLI) score, relevant disease description annotation, presence of previous database records, dbSNP rsID, and frequency in population were all considered at this step. For example, the *CHD7* variant identified for proband 1 had quality score of 448, pLI = 1.0, CHARGE syndrome annotation, splice donor functional effect, and allelic depth >10. The approximate number of candidate variants present at each major filtering step can be found in Table 2. These numbers have some flexibility, as several iterative approaches were performed on each trio and duo. Some filters were removed to check variants that may not have met all criteria but were still notable. In the case of the Proband 4 trio analysis 1 with proband/mother/father, the *APOB* variants were identified after scaling back the database occurrence filter. The final variants could be identified after increasing the filter from 5 to 10.

Full genomic coordinates and HGVS/HGVSp annotations can be found in Table S1. These were obtained by running the Variant Effect Predictor browser tool with the VCF entries for each variant as input.

3 | RESULTS

3.1 | Trio analyses

Demographics, clinical presentation, and identified mutations for proband and parent trios in our cohort are shown in Table 3. Deleterious mutations were identified in 6 of 7 probands studied. Table 4 includes DNA and RNA sample quality data and Table S1 includes variant data. Figure 1 displays family pedigrees.

3.1.1 | Family 1: *CHD7* mutation

Proband 1 was a male classified as nsCL/P and presented with a bilateral CLP, left hemifacial microsomia with facial nerve palsy, and an undescended testicle. Cardiac malformation included a hypoplastic aortic arch and Shone's complex: coarctation of the aorta and sub-aortic stenosis. The proband was found to have a de novo point mutation on chromosome 8 (NM_017780.4:c.3378 + 1G>A) for gene

CHD7. *CHD7* is a transcription regulator involved in chromatin remodeling. This particular mutation is expected to disrupt the splicing acceptor site. The variant is absent from gnomAD, however was classified as pathogenic according to the American College of Medical Genetics and Genomics and the Association for Medical Pathology (ACMG/AMP) criteria (Table 1) with mutations within the gene are known to be associated with CHARGE syndrome.

The *CHD7* gene often has novel variants, as was the case in this proband. Studies have found that *CHD7* gene mutations, which typically are distributed through coding exons resulting in early protein termination, can frequently possess variable phenotypic expressivity (Lalani et al., 2006). According to the most recently proposed diagnostic criteria for CHARGE syndrome, no major criteria of ocular coloboma, hypoplastic semi-circular canals, or choanal atresia were observed in this proband (Verloes, 2005). He underwent aortic arch augmentation at 5 days old followed by CL and CP repair at 11 months and 2.3 years, respectively. Follow-up to age three showed no growth abnormalities but developmental delay. Overall, this patient exhibited multiple minor criteria of CHARGE syndrome, including facial nerve palsy, congenital heart defect, and developmental delay (Verloes, 2005).

3.1.2 | Family 2: *SMARCA4* mutation

Proband 2 is a male that presented with an isolated CP, a hypoplastic aortic arch, and VSD. Cranial exam revealed multiple dental caries, diminished hearing, and a left eye larger than right. Other anomalies included a left inguinal hernia and right hydronephrosis. A de novo point mutation on chromosome 19 (NM_003072.5:c.2936G>A) was identified within the gene *SMARCA4*. This variant was classified as pathogenic according to ACMG/AMP criteria (Table 1). *SMARCA4* encodes for the BRG1 protein, which works in a SWI/SNF protein complex to regulate gene expression via ATP-dependent chromatin remodeling. An important component for cardiac development, *BRG1* deficiencies have been associated with midline cardiac defects consistent with the phenotype of tetralogy of Fallot (Qian et al., 2017). In this proband, the mutation created a missense of an actin-dependent transcription activator. The mutation has been associated with Coffin-Siris syndrome, which is defined by the presence of characteristic features that include developmental delay, fifth digit hypoplasia, and distinctive facial features of thick eyebrows, broad nasal bridge, and prominent philtrum (Fleck et al., 2001).

The proband underwent aortic arch reconstruction and VSD repair at 1 month of age, inguinal hernia repair at 2 months, and CP repair at age 2.1 years. At age seven, he exhibited normal speech but developmental delay. Aside from intellectual disability, no other features of Coffin-Siris syndrome were present in this proband.

3.1.3 | Family 3: *MED12* mutation

Proband 3 is a female that had a left CL and alveolus, bilateral preauricular pits, and diminished hearing. Cardiac malformations included

TABLE 2 Variant filtering for each candidate gene isolated

Proband analysis ^a	Quality filtered candidate variants ^b	Inheritance filtering ^c	Manual inspection of genes linked to phenotype
Trio Analysis: De novo (not in either parent), phased autosomal recessive, or X-linked			
Proband 1 Trio	184	De Novo (1): CHD7 (Splice Acceptor) Recessive (2): MAP1B(R1079Q);MAP1B(E1319K) X-linked (5): BRWD3(Q1551R) CDKL5(P947L); MUM1L1(D176N); SLITRK4(V719F);	De Novo (1): CHD7 (Splice Acceptor)
Proband 2 Trio	520	De Novo (1): CHD7 (Splice Acceptor) Recessive (2): SACS(T458I) + SACS(Q1143K) X-linked (0):	De Novo (1):SMARCA4
Proband 3 Trio	216	De Novo (1): MED12(c.3551delA[p.Q1184fs]) Recessive (0); X-linked (0):	De Novo (1): MED12
Proband 4 Trio	533	De Novo (0); X-linked (0): Recessive (10): AATK(P419H)/AATK(P1343T); APOB(F3753L)/APOB(E4256K) CELSR1 (E1499K)/CELSR1(G71R) PKD1(V882M)/PKD1 (V3850M) ZNF79(V165M)/ZNF79(R483Q)	Recessive: APOB(F3753L)/APOB (E4256K)
Duo Analysis: Inferred Phased Autosomal Recessive, Possible De Novo (Dominant negative), or X-linked			
Proband A Duo	189	Possible De Novo (25): ABR(A650T) ACAD9 (P259H) ADH5(A295P) AP2A1(D895N) BAIAP2L2(R292S); BAZ1A(T1382R) BEGAIN(P179L) CLIP2(R439K) CNTNAP4 (P134S) CSMD3(I2434V) DNAJC19(A2T) EGFLAM(S854P) GLDC(I91T) HID1(R204W) MCTP2(S680G) MOV10L1(N594H) RNASE4 (I90V) RNF213(S738N) SARS2(E210K) SEZ6 (S684L) TEX15(T2292M) VPS45(R386C) ZNF248(N115D) ZNF541(R417W) ZNF593 (S82C) Recessive (4): SETX(D448G) + SETX(S2497N) TTC40(G755R)/TTC40(L605P) X-linked (4): TLR8(P138S) AGTR2(G21V) GYG2 (G160R) TLR8(M1033K)	Recessive (2): SETX(D448G) + SETX (S2497N) Possible De Novo (1): RNF213(S738N)
Proband B Duo	237	Possible De Novo (37): AKAP11(I237V) AOX1 (L148M) ARHGDIB(D16N) ARHGEF39(C25*) ATCAY(E11G) CEP164(K322N) CLDN15 (G153R) COL4A2(G1468V) CSN3(H90Q) CTSE(G80S) DIP2A(S59P) ENPP6(G344V) FHOD3(E638K) IGF2BP1(Q226H) JAG1 (N1187S) KIAA1614(S421C) LAYN(L93P) LIFR(N680D) LRIG1(L843F) LRRC27(W360*) MCM5(S142L) MICALL2(S94N) MOV10 (W277R) PER3(S355R) PIEZO1(T476M) POLG(L594V) PRRT4(G693D) PTPLAD1 (S325F) RAD54L(R320G) RBMXL2(P160H) ROBO1(N1372K) SLC35G6(N129D) SQLE(S232R) STX6(M106I) TDP1(D407G) TUBE1(M349V) TYK2(K1175N) Recessive (2): DISC1(T603M) + DISC1(P2L)	Possible De Novo (1): JAG1(N1187S)

^aTrio indicates mother/father/affected. Duo indicates Mother/Child (father unavailable).

^bQuality Filtered Candidate Variants were *moderate* or *high* predicted functional impact using SNPeff; GATK quality score >300, have a MAF of <1% in major population databases found in dbNSFP3.0. Genes flagged for false positives were excluded (paralogs, etc.). Variants found at high frequency in internal databases were excluded, as were multiallelic insertion/deletions within a single family. Finally, homozygous variants in parents or variants with same genotype in all family members were excluded.

^cFamily Trio's were available for Proband 1–4. For these, variants were filtered by inheritance: (a) de novo (not in either parent), (b) phased autosomal recessive pairs, or (c) X-linked inherited maternally and outside of the pseudo-autosomal region. For Duo's, phasing was inferred using one parent. A category for possible De Novo was where one variant where a heterozygote variant is not found in the parent and the variant is not found in major population databases.

TABLE 3 Genetic variant and clinical characteristics of patient trios (1–4) and duos (A–C)

Proband	Age	Gender	Race (ethnicity)	Genetic mutation	Cleft diagnosis	Cardiac diagnosis	Other defects	Family history
1	7	M	Other (Hispanic)	<i>CHD7</i>	Bilateral CLP	Arch, Shone's complex	Hemifacial microsomia, undescended testicle	None
2	8	M	White (Hispanic)	<i>SMARCA4</i>	iCP	Arch, VSD	Multiple dental caries, hearing loss, ocular asymmetry, inguinal hernia, hydronephrosis	None
3	4	F	White (Hispanic)	<i>MED12</i>	Left CL and alveolus	Arch, VSD	Bilateral preauricular pits, hearing loss, ectopic ureters, hydronephrosis, intestinal malrotation with Ladd bands	None
4	5	F	Black (African American)	<i>APOB</i>	Left CLP	DORV, I-TGA, dextrocardia, HRV	Right anophthalmia, central hypothyroidism, absent corpus callosum, occipital skull defect, hydrocephalus	Twin sister with DORV, unbalanced AV canal, HLV
A	3	M	White (Hispanic)	<i>RNF213</i> and <i>SETX</i>	Bilateral CLP	TOF	Global developmental delay, dysplastic ears	None
B	20	M	White (Hispanic)	<i>JAG1</i>	SMCP	TOF	right cryptorchidism, imperforate anus, hypoparathyroidism, and seizure disorder	None
C	5	M	Pacific Islander	None	Left CLP	TOF	Polydactyly	None

Abbreviations: Arch, hypoplastic aortic arch; AV, aortic valve; CL, cleft lip; CLP, cleft lip and palate; DORV, double outlet right ventricle; HLV, hypoplastic left ventricle; HRV, hypoplastic right ventricle; iCP, isolated cleft palate; I-TGA, transposition of the great arteries; SMCP, submucous cleft palate; TOF, tetralogy of fallot; VSD, ventricular septal defect.

a hypoplastic aortic arch with VSD. Other anomalies included ectopic ureters with bilateral hydronephrosis and intestinal malrotation with Ladd bands. Sequencing identified a de novo frame shift mutation on the paternal X-chromosome (NM_005120.3:c.3551del) within the *MED12* gene, defined as pathogenic according to ACMG/AMP criteria (Table 1). In this proband, mRNA analysis revealed skewed X-inactivation of her maternal chromosome. This is suggestive of the presence of an additional abnormality on the opposing allele that ultimately leads to heterozygous phenotypic expression.

MED12, which encodes the mediator complex subunit 12, serves as a transcription factor for RNA polymerase and thus plays an important role in gene expression (U.S. National Library of Medicine, 2020a; *MED12* gene). While the mutation in this proband was unknown to gnomAD, multiple syndromes have been associated with gene mutations in *MED12*: Opitz-Kaveggia syndrome, Lujan-Fryns syndrome, and Odho syndrome (Ding et al., 2008; Rubinato et al., 2020). Lujan-Fryns syndrome is an x-linked recessive disorder classically described in males who demonstrate marfanoid body habitus, macrocephaly, narrow face, maxillary hypoplasia, arched palate, high nasal root, and hypotonia (Van Buggenhout & Fryns, 2006). Odho syndrome has reported cleft as an uncommon phenotype (Caro-Llopis et al., 2016). None of the known associated syndromes have reported CHD.

The proband underwent aortic arch augmentation and PFO closure at 12 days old, CL and alveolus repair at 4 months, reduction of midgut volvulus at 7 months, and re-implantation of ectopic ureters at 2 years. At age three, the proband exhibited developmental and speech delay. With exception of developmental delay, this proband had no other major characteristic features of Lujan-Fryns syndrome.

3.1.4 | Family 4: *APOB* mutation

Proband 4 is a female with unilateral, left-sided CL and CP, right anophthalmia, central hypothyroidism, absent corpus callosum, and a right occipital skull defect with hydrocephaly at birth. Cardiac malformations in the proband included DORV, I-TGA, dextrocardia, and hypoplastic right ventricle. The proband was found to have two de novo point mutations on chromosome 2 within the gene for Apolipoprotein B (*APOB*). The protein, which can lead to the development of atherosclerotic plaques in cardiovascular disease, is not known to be associated with cardiac developments (Shapiro & Fazio, 2017). The first variant (NM_000384.3:c.12766G>A) is of unknown significance according to AMG/AMP criteria and known to generate a missense mutation in the lipid transporter. The second variant (NM_000384.3:

TABLE 4 Genomic sequencing sample characteristics

ID	DNA					RNA								
	M reads mapped	% aligned	Insert size (bp)	% duplicates	% > = Q30 bases	Mean quality score	Yield (Mbases)	M reads mapped	% rRNA	% mRNA	% aligned	Insert size	% dups	M aligned
Proband 1	1287	100%	427	9.60%	90.8%	35.4	116,836							
Proband 1 mother	1113	100%	414	9.00%	90.3%	35.3	99,793							
Proband 1 father	1197	100%	414	9.50%	91.3%	35.5	123,393							
Proband 2	1747	100%	413	9.70%	91.2%	35.5	200,816							
Proband 2 mother	1214	100%	434	9.40%	91.6%	35.5	183,172							
Proband 2 father	1463	100%	429	9.50%	90.7%	35.4	130,097							
Proband 3	1367	100%	438	9.50%	90.7%	35.4	120,341	624.8	6.20%	82.70%	96%	212 bp	62.30%	102.2
Proband 3 mother	933	100%	447	9.40%	90.9%	35.4	140,870							
Proband 3 father	1205	100%	432	9.90%	91.2%	35.5	181,846							
Proband 4	1370	100%	448	9.40%	90.9%	35.4	206,933	971.2	1.20%	90.30%	95%	226 bp	62.20%	160.5
Proband 4 mother	3235	100%	440	10.40%	90.9%	35.4	488,915							
Proband 4 father	2323	100%	442	10.30%	91.1%	35.4	350,605							
Proband 4 twin +CHD/-cleft	1828	100%	440	10.10%	91.3%	35.5	276,009							
Proband 4 twin -CHD/-cleft	3620	100%	431	10.90%	91.2%	35.5	546,714							
Proband A	2166	99%	432	10.70%	90.9%	35.4	328,149							
Proband A mother	1141	100%	432	9.80%	91.2%	35.5	172,279							
Proband B	1162	100%	428	9.60%	90.8%	35.4	126,612							
Proband B mother	1216	100%	423	9.70%	90.9%	35.4	143,654							
Proband C	1161	100%	440	9.30%	90.6%	35.4	109,473							
Proband C father	1159	100%	439	8.70%	90.9%	35.4	107,107							

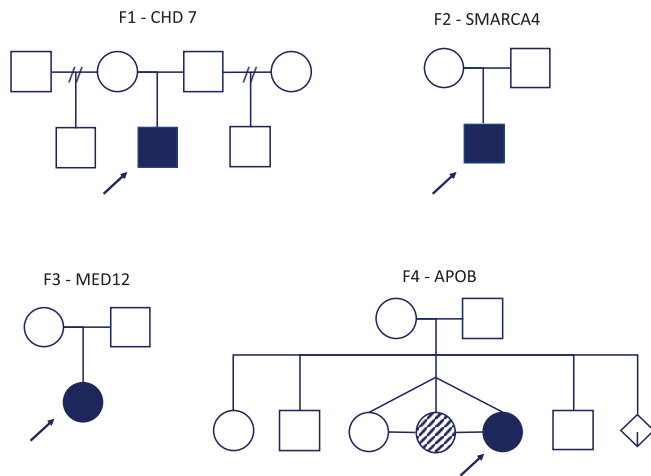


FIGURE 1 Four pedigrees of proband families. Family number and mutated gene marked above the pedigree (F# - gene). Solid black gender symbols indicate combined phenotype of CHD and CL/P. striped gender symbol indicates CHD only phenotype. An arrow marks the proband in each family

c.11257T>C) generates a second missense mutation of unknown significance.

The proband (triplet C) had two triplet siblings (A and B) all born at 32-weeks' gestation. Triplet B (monoamniotic) had DORV, unbalanced AV canal, and hypoplastic left ventricle, but no craniofacial anomalies. Triplet A (diamniotic) had neither craniofacial nor cardiac anomalies. All three triplets underwent sequencing and were found to be genetically identical. Both de novo variants were shared between the proband and her two triplet siblings. As *APOB* is not routinely expressed in blood, mRNA analysis did not reveal any differential expression patterns between the proband and her siblings.

The proband underwent cardiac surgery at ages 22 months and 5 years. Her CL and CP repairs occurred at ages 2.5 and 3 years, respectively. Follow-up to age five revealed eczema, stunted growth, and developmental delay in the proband and normal growth in the two triplet siblings. All three triplets had umbilical hernias repaired at age three. A younger brother to the proband has psoriasis (Figure 1).

3.2 | Duo analyses

Of the three proband and parent duos, two (67%) demonstrated a total of three genetic variants (Table S1). All three probands had a cardiac diagnosis of TOF.

3.2.1 | Duo family a: RNF213 and SETX mutations

The proband presented with a bilateral complete CLP. Other anomalies included global developmental delay and mildly dysplastic ears. Three heterozygous missense variants were identified in two genes for this proband: *RNF213* and *SETX*. The *RNF213* variant was on

chromosome 17 (NM_020954.4:c.2213G>A). *RNF213* gene mutations have previously been associated with Moyamoya disease, characterized by vascular maturation defects and cerebrovascular disease. Two variants were identified in the *SETX* gene on chromosome 9 (NM_001351527.2:c.7490G>A and NM_001351527.2:c.1343A>G). All variants are of unknown significance per ACMG/AMP classifications. Mutations in *SETX* have previously been associated with neuromuscular and neurologic disorders, including Juvenile Amyotrophic Lateral Sclerosis and Spinocerebellar Ataxia. Phenotypes associated with these previously described *RNF213* and *SETX* genetic syndromes were not observed in this proband. Our proband underwent TOF repair at 7 months, CL and alveolus repair at 15 months, and CP repair at 2.5 years. At age three, the proband exhibited persistent developmental and speech delay.

3.2.2 | Duo family B: JAG1 mutation

Proband B presented with submucous CP at age 11. Other anomalies included right cryptorchidism, imperforate anus, hypoparathyroidism, and seizure disorder. A *JAG1* variant of unknown significance was identified (NM_000214.3:c.3560A>G). Prior studies have described *JAG1* mutations in the context of Allagille Syndrome, which is associated with intrahepatic ductal defects, hypertelorism, vertebral abnormalities, and distinctive facial features that include broad forehead and pointed chin as an infant and broad chin as they age. Such phenotypes were not observed in this proband. His TOF repair occurred by 6 months of age, anoplasty in early childhood, cryptorchidism at age 10, and CP repaired at age 12. By age 19, his hypoparathyroidism and seizures were well managed medically.

3.2.3 | Duo family C

Proband C presented with bilateral CLP in addition to right hand pre-axial polydactyly and failure to thrive. Patient did not have any other dysmorphic features. His CL repair occurred at 6 months old, TOF repair at 8 months, G-tube placement at 12 months, CP repair at 16 months, and polydactyly repair at 5 years. At age 5, the patient was behaving appropriately for age. No gene variants of sufficient quality were identified in this proband parent duo.

3.3 | Gene ontology and pathway analysis

To better understand the molecular function and signaling pathways associated with the identified variants, an exploratory gene ontology and pathway analysis was performed of all seven candidate genes identified in trio and duo probands (Table S1). This analysis was performed using a combination of PANTHER, DAVID web-based software, and a primary literature search. The most common biological processes ascribed to these variants included regulation of RNA polymerase II activity (71.4%), nervous system development (42.9%), heart

morphogenesis (28.6%), chromatin remodeling (28.6%), and angiogenesis (28.6%). Predictive analysis of variant functions demonstrated that 42.9% of genes were involved in regulation of transcription (42.9%). With regards to cellular signaling pathways, 4/7 (57%) gene variants (*CHD7*, *SMARCA4*, *MED12*, and *RNF213*) were predicted and/or previously demonstrated to be involved in the Wnt-signaling pathway in addition to other individual gene involvements (Al-Hendy et al., 2017; Amal et al., 2019; Griffin et al., 2011). Other molecular functions, biological processes, and pathways of relevance are shown in Figure 2. In addition to assessing associated molecular and pathway functions, we evaluated which of the seven genes have been shown to be expressed in murine embryonic tissues associated with craniofacial and cardiac development. RNA in situ hybridization and RNA-seq performed on E9.5 to E14.5 mouse embryos demonstrate that *Chd7*, *Smarca4*, *Med12*, *Rnf213*, *Setx*, and *Jag1* are transcriptionally expressed in both first brachial arch artery and cardiac tissues, supporting the assertion that these genes may be implicated in mechanisms of orofacial clefting and CHD (Brunskill

et al., 2014; Cardoso-Moreira et al., 2019; Hooper et al., 2017; Loomes et al., 1999).

4 | DISCUSSION

Advances in next generation sequencing platforms have accelerated efforts to investigate the genetic etiology of congenital birth defects. One approach has been to identify de novo rare variant mutations through comparative whole exome sequencing (WES) in patient-parent trios of all comers with congenital defects. While this approach has been informative for exploring the genomic architecture underlying different types of congenital defects, the yield of causative lesion-specific candidate genes has been relatively small. For example, WES analysis in patients with any form of CHD demonstrated de novo mutations in only 10% of patients (Homsy et al., 2015; Zaidi et al., 2013). An alternative approach is to perform genomic analyses

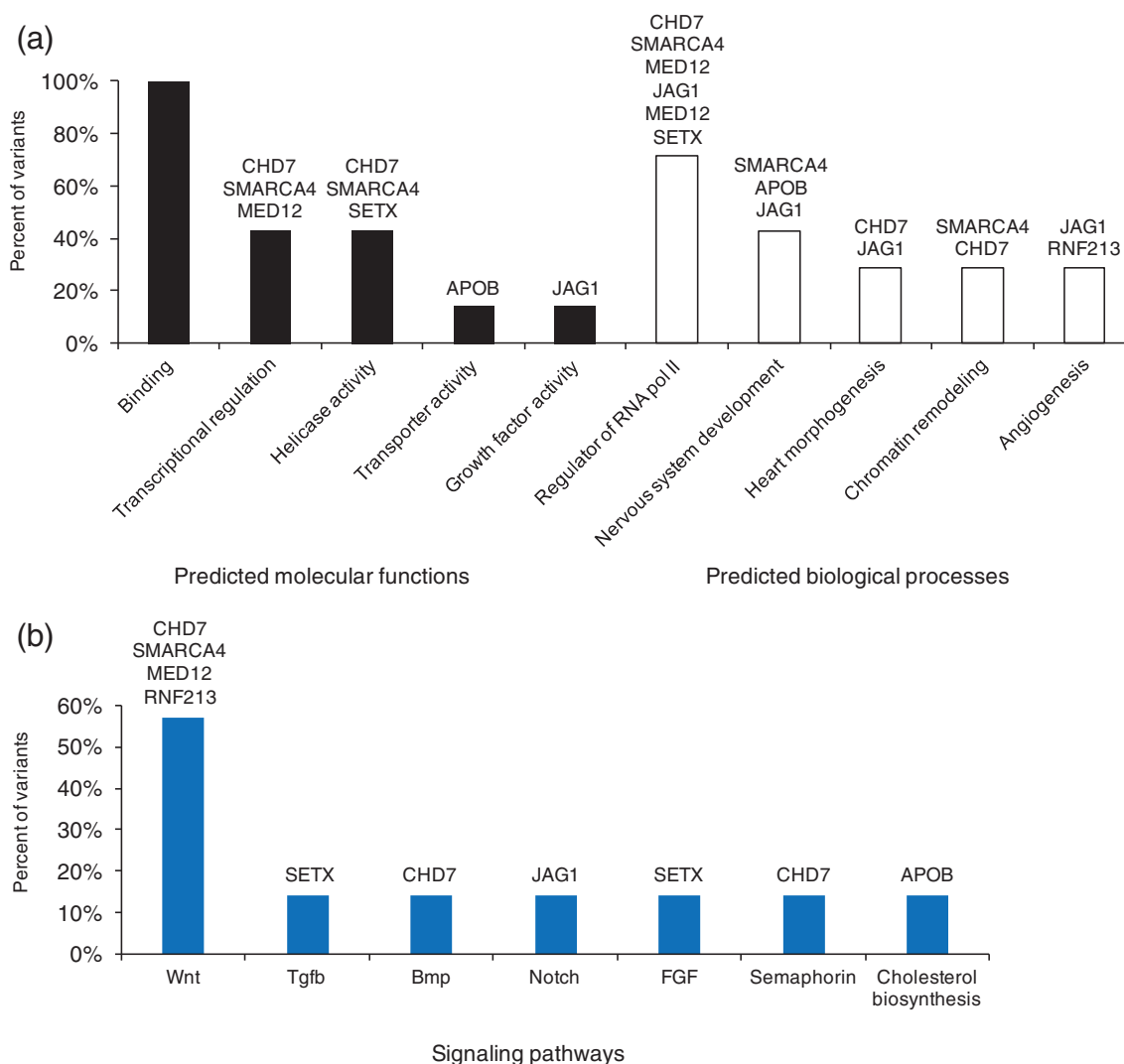


FIGURE 2 Predicted (a) molecular functions and biological processes and (b) associated signaling pathways of de novo variants identified in nsCHD+CL/P probands

in a prespecified niche patient population enriched either by homogeneous phenotypes or by co-existing abnormalities. This approach capitalizes on the expectation that the incidence of genetic defects would be higher in a preselected population. In support of this approach, when CHD patients with neurodevelopmental abnormalities were selectively evaluated, pathogenic de novo mutations were identified in almost a third of the patients (Homsy et al., 2015).

Our group is the first to demonstrate enrichment of CHD, particularly OFT lesions, in patients with CL/P. We hypothesized that the increase in concomitant presentation likely results from derangements in a common developmental paradigm. We therefore undertook the current analysis to evaluate the prevalence of genetic variants in a small pilot cohort of patients with nsCL/P and OFT CHD. All four patients included in the trio evaluation and three patients in duo evaluation had negative chromosomal microarrays but all, but one, were found to harbor protein-damaging mutations. In contrast, a study of 1200 CHD trios with a spectrum of concomitant birth defects found only 20% prevalence of de novo mutations (Jin et al., 2017). The high prevalence of deleterious mutations in our cohort further suggests a more highly conserved shared developmental pathway between cleft and OFT cardiac defects.

The availability of proband-parent trios in four cases allowed us to identify de novo mutations with very high certainty. Of the four genes with variants identified, only one (*CHD7*) has been known to be implicated in both CL/P and CHD. While CHD is common in patients with CHARGE syndrome, appearing in up to 91% of cases, cleft defects are less common at 15%–30% (Isaac et al., 2018; Lalani et al., 2006; van Ravenswaaij-Arts et al., 1993). In patients classified as having nsCL/P, *CHD7* variants are an even more uncommon occurrence (Felix et al., 2006). Therefore, based on different diagnostic criteria, the proband identified with a de novo *CHD7* mutation could be clinically identified as having possible CHARGE syndrome, but often times, as in our case, may be identified as nondiagnostic (Blake et al., 1998; Jongmans et al., 2006; Verloes, 2005).

The de novo mutations in *SMARCA4* and *MED12* seen in two of the probands were identified as pathogenic in our cases and are known to be associated with syndromic conditions. Up to 50% of patients with *SMARCA4* mutations have been reported to have a CP and 42% a cardiovascular complication (Kosho et al., 2014; Tsurusaki et al., 2014). However, the frequency of overlapping phenotypes has not been reported. The most common syndrome associated with *SMARCA4* gene mutations is Coffin–Siris Syndrome, which classically presents with developmental delay, ulnar digit abnormalities, and coarse facial features, of which only intellectual disability was observed in our patient (U.S. National Library of Medicine, 2020b; *SMARCA4* gene).

For *MED12*, our proband was unique in that she is female and demonstrated heterozygous expression of a typically x-linked variant. In a small case series, additional *MED12* variants have been found to have an expanded phenotypic presentation including female probands, one of whom had CP without CHD and three who had CHD but no orofacial clefting. Our proband, who expressed a variant

resulting in a frameshift mutation, may have a more deranged protein structure accounting for the variable and combined phenotype.

APOB, a gene that encodes for apolipoprotein B, the main component of chylomicrons, presented as a surprising variant in one proband and her triplet siblings. Studies have found indirect associations between *APOB* and CHD—maternal derangement in expression of *APOB* is associated with increased rates of CHD in their offspring, particularly VSD, tetralogy of Fallot, and pulmonary valve stenosis (Smedts et al., 2012). HLHS, as seen in our proband and sibling, was less common but still observed. No evidence, however, has suggested that self-expression of de novo *APOB* mutations confers increased risk of CHD. Additionally, while the *APOB* double-missense mutation was present in all three triplets, CHD was only observed in 2, and CL/P only seen in the proband. No studies have reported *APOB* mutations associated with orofacial cleft defects. Without a tissue sample to evaluate *APOB* protein levels, this study is limited in understanding how expressivity may have varied between the proband and her siblings.

The ability to identify truly de novo pathogenic mutations is limited in the subset of patients presenting as duo samples. Despite this limitation, mutations identified in duo probands and absent in their respective parents were still mechanistically revealing. One duo was found to have heterozygous missense variants in two separate genes, *RNF213* and *SETX*. *RNF213* gene codes for a protein with E3 ubiquitination and ATPase functions and has previously been identified as an important genetic susceptibility gene in Moyamoya syndrome (Fujimara et al., 2016). Moyamoya syndrome is characterized as a chronic occlusive vascular disease that is predominately associated with cerebrovascular pathologies. While *RNF213* gene mutations have not yet been described in patients with CL/P or CHD, such mutations have recently been described in patients with midaortic syndrome and pulmonary artery stenosis, suggesting that *RNF213* may have implications in regulating vascular biology more generally (Chang et al., 2018; Warejko et al., 2018).

SETX is an RNA/DNA helicase that has been associated with ataxia with oculomotor apraxia type 2 and amyotrophic lateral sclerosis type 4 (Groh et al., 2017). Mechanistically, *SETX* functions as a regulator of transcription. *SETX* gene mutations have not been described in CHD or CL/P. However, *SETX* has been shown to interact with transcriptional regulatory proteins with known associations with heart and palatal development, including RNA polymerase II, *CHD4*, and Histone H3/H4 (Ji et al., 2020; Loenarz et al., 2010; Schwenty-Lara et al., 2020; Zaidi et al., 2013). The second duo had a variant of unknown significance in *JAG1*, the gene causative for Alagille syndrome. *JAG1* is a putative ligand of the Notch signaling pathway, which is an established signaling pathway with relevance in both congenital palatal and cardiac pathologies (Casey et al., 2006; Dezoysa et al., 2020). Alagille syndrome includes biliary malformations and pulmonary artery defects, but has also been associated with Tetralogy of Fallot, as seen in the proband harboring the *JAG1* variant in our sample (Bauer et al., 2010).

An important limitation of our analysis is the small sample size of this inception cohort. It is not possible to execute statistically sound

pathway and ontology enrichment analyses to reach definitive conclusions given the limited number of patients. Yet, we submit that our pilot analysis has the potential to provide early mechanistic insights that could guide future studies in larger patient cohorts. To that end, we sought to investigate the biologic relationship between gene candidates using a molecular and pathway-level analysis. Using gene ontology assessment and primary literature search, we demonstrate that the majority of candidate variants is involved in binding and transcriptional regulation, which points toward a common biologic functionality across variants. At the pathway level, our analysis discovered that 57% of variants have some known association with the Wnt signaling pathway. The Wnt signaling pathway is an evolutionarily conserved pathway with established roles in cardiac and craniofacial development. Preclinical investigations in murine models have shown that the genetic deletion of Wnt pathway genes during embryonic development results in cardiac and orofacial phenotypes similar to those observed in this CHD and nsCL/P cohort (He et al., 2008; He et al., 2011; Schleiffarth et al., 2007; Sinha et al., 2012). Lack of target palate or heart tissue limited our ability to validate protein level findings in our cohort. Additionally, owing to a significant loss of tolerance of deleterious gene mutations in putative members of the Wnt pathway, such genetic variants have not routinely been described in the literature. Our data suggest that loss-of-function variants in genetic modifiers or downstream Wnt signaling molecules may serve as a common molecular basis for combined congenital cardiac and cleft defects in humans.

5 | CONCLUSIONS

Our pilot analysis of a small cohort of patients with combined CL/P and OFT CHD phenotype suggests a potentially significant prevalence of deleterious mutations. An overrepresentation of mutations in molecules associated with the Wnt-signaling pathway appears to exist. Many of these variants are associated with known syndromes, suggesting that syndromic conditions associated with CL/P and OFT CHD may have greater phenotypic variability than previously appreciated. Further studies, particularly with trio exome or genome sequencing in larger cohorts of patients are needed to understand the mechanistic implications of these mutations and the developmental derangements that result in concomitant CL/P and OFT CHD.

ACKNOWLEDGMENT

We acknowledge and appreciate the participation of our study patients and their families.

CONFLICT OF INTEREST

The authors have no conflicts of interest to disclose.

AUTHOR CONTRIBUTIONS

Naikhoba C.O. Munabi contributed to study conception, study design, patient selection, sample acquisition, interpretation of data, and

drafting and revising the manuscript. Shady Mikhail contributed to patient selection, sample acquisition, and drafting the manuscript. Omar Toubat contributed to interpretation of data and drafting and revising the manuscript. Michelle Webb contributed to genomic sequencing, interpretation of data, and revising the manuscript. Allyn Auslander contributed to study conception, study design, patient selection, sample acquisition, and revising the manuscript. Pedro A. Sanchez-Lara and Ryan J. Schmidt contributed to study conception, study design, patient selection, interpretation of data, and revising the manuscript. Zarko Manojlovic and David Craig contributed to study design, sample acquisition, genomic sequencing, interpretation of data, drafting, and revising the manuscript. William P. Magee III contributed to study conception, study design, patient selection, sample acquisition, and revising the manuscript. S. Ram Kumar contributed to study conception, study design, patient selection, interpretation of data, and drafting and revising the manuscript. All authors reviewed and approved of the final published version.

DATA AVAILABILITY STATEMENT

The data that support the findings of this study are available from the corresponding author upon reasonable request.

ORCID

Naikhoba C. O. Munabi  <https://orcid.org/0000-0003-2731-837X>

Subramanyan Ram Kumar  <https://orcid.org/0000-0003-1487-4203>

REFERENCES

- Aldrich, J. (2020). Github.tgen/tCoNuT: GitHub. Retrieved from <https://github.com/tgen/tCoNuT>.
- Al-Hendy, A., Laknaur, A., Diamond, M. P., Ismail, N., Boyer, T. G., & Halder, S. K. (2017). Silencing Med12 gene reduces proliferation of human leiomyoma cells mediated via Wnt/ β -catenin signaling pathway. *Endocrinology*, 158(3), 592–603. <https://doi.org/10.1210/en.2016-1097>
- Amal, H., Gong, G., GJoneska, E., Lewis, S. M., Wishnok, J. S., Tsai, L., & Tannenbaum, S. R. (2019). S-nitrosylation of E3 ubiquitin-protein ligase RNF213 alters non-canonical Wnt/Ca²⁺ signaling in the P301S mouse model of tauopathy. *Translational Psychiatry*, 9, 44. <https://doi.org/10.1038/s41398-019-0388-7>
- Arth, A. C., Tinker, S. C., Simeone, R. M., Ailes, E. C., Cragan, J. D., & Grosse, S. D. (2017). Inpatient hospitalization costs associated with birth defects among persons of all ages—United States, 2013. *MMWR. Morbidity and Mortality Weekly Report*, 66(2), 41–46. <https://doi.org/10.15585/mmwr.mm6602a1>
- Azadgoli, B., Munabi, N. C. O., Fahradyan, A., Auslander, A., McCullough, M., Aflatooni, N., Ward, S. L. D., Kumar, S. R., Sanchez-Lara, P. A., Swanson, J., & Magee, W. P., 3rd. (2020). Congenital heart disease in patients with cleft lip/palate and its impact on cleft management. *The Cleft Palate-Craniofacial Journal*, 57(8), 957–966. <https://doi.org/10.1177/1055665620924915>
- Bauer, R. C., Laney, A. O., Smith, R., Gerfen, J., Morrisette, J. J. D., Woyciechowski, S., Garbarini, J., Loomes, K. M., Krantz, I. D., Urban, Z., Gelb, B. D., Goldmuntz, E., & Spinner, N. B. (2010). Jagged1 (Jag1) mutations in patients with tetralogy of Fallot or pulmonary stenosis. *Human Mutation*, 31(5), 594–601. <https://doi.org/10.1002/humu.21231>
- Blake, K. D., Davenport, S. L., Hall, B. D., Hefner, M. A., Pagon, R. A., Williams, M. S., Lin, A. E., & Graham, J. M., Jr. (1998). CHARGE association: An update and review for the primary pediatrician. *Clinical*

- Pediatrics (Phila)*, 37(3), 159–173. <https://doi.org/10.1177/00092289803700302>
- Brunskill, E. W., Potter, A. S., Distasio, A., Dexheimer, P., Plassard, A., Aronow, B. J., & Potter, S. S. (2014). A gene expression atlas of early craniofacial development. *Developmental Biology*, 391(2), 133–146. <https://doi.org/10.1016/j.ydbio.2014.04.016>
- Cardoso-Moreira, M., Halbert, J., Valloton, D., Velten, B., Chen, C., Shao, Y., Liechti, A., Ascensão, K., Rummel, C., Ovchinnikova, S., Mazin, P. V., Xenarios, I., Harshman, K., Mort, M., Cooper, D. N., Sandi, C., Soares, M. J., Ferreira, P. G., Afonso, S., ... Kaessmann, H. (2019). Gene expression across mammalian organ development. *Nature*, 571(7766), 505–509. <https://doi.org/10.1038/s41586-019-1338-5>
- Caro-Llopis, A., Rosello, M., Orellana, C., Oltra, S., Monfort, S., Mayo, S., & Martinez, F. (2016). De novo mutations in genes of mediator complex causing syndromic intellectual disability: Mediatoropathy or transcriptomopathy? *Pediatric Research*, 80(6), 809–815. <https://doi.org/10.1038/pr.2016.162>
- Casey, L. M., Lan, Y., Cho, E. S., Maltby, K. M., Gridley, T., & Jiang, R. (2006). Jag2-Notch1 signaling regulates oral epithelial cell differentiation and palate development. *Developmental Dynamics*, 235(7), 1830–1844. <https://doi.org/10.1002/dvdy.20821>
- Centers for Disease Control and Prevention. (2019). *Infant Mortality*. Retrieved from <https://www.cdc.gov/reproductivehealth/maternalinfanthealth/infantmortality.htm>.
- Chang, S. A., Song, J. S., Park, T. K., Yang, J. H., Kwon, W. C., Kim, S. R., Kim, S. M., Cha, J., Jang, S. Y., Cho, Y. S., Kim, T. J., Bang, O. Y., Song, J. Y., Ki, C. S., & Kim, D. K. (2018). Nonsyndromic peripheral pulmonary artery stenosis associated with homozygosity of RNF213 p.Arg4810Lys regardless of co-occurrence of moyamoya disease. *Chest*, 153(2), 404–413. <https://doi.org/10.1016/j.chest.2017.09.023>
- DePristo, M. A., Banks, E., Poplin, R., Garimella, K. V., Maguire, J. R., Hartl, C., Philippakis, A. A., del Angel, G., Rivas, M. A., Hanna, M., McKenna, A., Fennell, T. J., Kernytsky, A. M., Sivachenko, A. Y., Cibulskis, K., Gabriel, S. B., Altshuler, D., & Daly, M. J. (2011). A framework for variation discovery and genotyping using next-generation DNA sequencing data. *Nature Genetics*, 43(5), 491–498. <https://doi.org/10.1038/ng.806>
- DeZoysa, P., Liu, J., Toubat, O., Choi, J., Moon, A., Gill, P. S., Duarte, A., Sucov, H. M., & Kumar, S. R. (2020). Delta-like ligand 4-mediated notch signaling controls proliferation of second heart field progenitor cells by regulating Fgf8 expression. *Development*, 147(17), dev185249. <https://doi.org/10.1242/dev.185249>
- Ding, N., Zhou, H., Esteve, P. O., Chin, H. G., Kim, S., Xu, X., Joseph, S. M., Friez, M. J., Schwartz, C. E., Pradhan, S., & Boyer, T. G. (2008). Mediator links epigenetic silencing of neuronal gene expression with x-linked mental retardation. *Molecular Cell*, 31(3), 347–359. <https://doi.org/10.1016/j.molcel.2008.05.023>
- Dobin, A., Davis, C. A., Schlesinger, F., Drenkow, J., Zaleski, C., Jha, S., Batut, P., Chaisson, M., & Gingeras, T. R. (2013). STAR: Ultrafast universal RNA-seq aligner. *Bioinformatics*, 29(1), 15–21. <https://doi.org/10.1093/bioinformatics/bts635>
- Felix, T. M., Hanshaw, B. C., Mueller, R., Bitoun, P., & Murray, J. C. (2006). CHD7 gene and non-syndromic cleft lip and palate. *American Journal of Medical Genetics. Part A*, 140(19), 2110–2114. <https://doi.org/10.1002/ajmg.a.31308>
- Fleck, B. J., Pandya, A., Vanner, L., Kerkering, K., & Bodurtha, J. (2001). Coffin-Siris syndrome: Review and presentation of new cases from a questionnaire study. *Journal of Medical Genetics*, 99(1), 1–7. [https://doi.org/10.1002/1096-8628\(20010215\)99:1<1::aid-ajmg1127>3.0.co;2-a](https://doi.org/10.1002/1096-8628(20010215)99:1<1::aid-ajmg1127>3.0.co;2-a)
- Fujimara, M., Bang, O. Y., & Kim, J. S. (2016). Moyamoya disease. *Frontiers of Neurology and Neuroscience*, 40, 204–220. <https://doi.org/10.1159/000448314>
- Griffin, C. T., Curtis, C. D., Davis, R. B., Muthukumar, V., & Magnuson, T. (2011). The chromatin-remodeling enzyme BRG1 modulates vascular Wnt signaling at two levels. *Proceedings of the National Academy of Sciences of the United States of America*, 108(6), 2282–2287. <https://doi.org/10.1073/pnas.1013751108>
- Groh, M., Albulescu, L. O., Cristini, A., & Gromak, N. (2017). Senataxin: Genome guardian at the interface of transcription and neurodegeneration. *Journal of Molecular Biology*, 429(21), 3181–3195. <https://doi.org/10.1016/j.jmb.2016.10.021>
- Grygiel-Gorniak, B., Oduah, M. T., Olagunju, A., & Klokner, M. (2020). Disorders of the aorta and aortic valve in connective tissue diseases. *Current Cardiology Reports*, 22(8), 70. <https://doi.org/10.1007/s11886-020-01314-0>
- He, F., Xiong, W., Wang, Y., Li, L., Liu, C., Yamagami, T., Taketo, M. M., Zhou, C., & Chen, Y. (2011). Epithelial Wnt/ β -catenin signaling regulates palatal shelf fusion through regulation of Tgf β 3 expression. *Developmental Biology*, 350(2), 511–519. <https://doi.org/10.1016/j.ydbio.2010.12.021>
- He, F., Xiong, W., Yu, X., Espinoza-Lewis, R., Liu, C., Gu, S., Nishita, M., Suzuki, K., Yamada, G., Minami, Y., & Chen, Y. (2008). Wnt5a regulates directional cell migration and cell proliferation via Ror2-mediated non-canonical pathway in mammalian palate development. *Development (Cambridge, England)*, 135(23), 3871–3879. <https://doi.org/10.1242/dev.025767>
- Heron, M. (2016). Deaths: Leading causes for 2014. *National Vital Statistics Reports*, 65(5), 1–96.
- Homsy, J., Zaidi, S., Shen, Y., Ware, J. S., Samocha, K. E., Karczewski, K. J., DePalma, S. R., McKean, D., Wakimoto, H., Gorham, J., Jin, S. C., Deanfield, J., Giardini, A., Porter, G. A., Jr., Kim, R., Bilguvar, K., López-Giráldez, F., Tikhonova, I., Mane, S., ... Chung, W. K. (2015). De novo mutations in congenital heart disease with neurodevelopmental and other congenital anomalies. *Science*, 350(6265), 1262–1266. <https://doi.org/10.1126/science.aac9396>
- Hooper, J. E., Feng, W., Li, H., Leach, S. M., Phang, T., Siska, C., Jones, K. L., Spritz, R. A., Hunter, L. E., & Williams, T. (2017). Systems biology of facial development: Contributions of ectoderm and mesenchyme. *Developmental Biology*, 426(1), 97–114. <https://doi.org/10.1016/j.ydbio.2017.03.025>
- Isaac, K. V., Ganske, I. M., Rottgers, S. A., Lim, S. Y., & Mulliken, J. B. (2018). Cleft lip and palate in CHARGE syndrome: Phenotypic features that influence management. *The Cleft Palate-Craniofacial Journal*, 55(3), 342–347. <https://doi.org/10.1177/1055665617738994>
- Ji, W., Ferdman, D., Copel, J., Scheinost, D., Shabanova, V., Brueckner, M., Khokha, M., ... K., & Ment, L. R. (2020). De novo damaging variants associated with congenital heart diseases contribute to the connectome. *Scientific Reports*, 10(1), 7046. <https://doi.org/10.1038/s41598-020-63928-2>
- Jin, S. C., Homsy, J., Zaidi, S., Lu, Q., Morton, S., DePalma, S. R., Zeng, X., Qi, H., Chang, W., Sierant, M. C., Hung, W. C., Haider, S., Zhang, J., Knight, J., Bjornson, R. D., Castaldi, C., Tikhonova, I. R., Bilguvar, K., Mane, S. M., ... Brueckner, M. (2017). Contribution of rare inherited and de novo variants in 2,871 congenital heart disease probands. *Nature Genetics*, 49(11), 1593–1601. <https://doi.org/10.1038/ng.3970>
- Jongmans, M. C., Admiraal, R. J., van der Donk, K. P., Vissers, L. E., Baas, A. F., Kapusta, L., van Hagen, J. M., Donnai, D., de Ravel, T. J., Veltman, J. A., Geurts van Kessel, A., De Vries, B. B., Brunner, H. G., Hoefsloot, L. H., & van Ravenswaaij, C. M. (2006). CHARGE syndrome: The phenotypic spectrum of mutations in the CHD7 gene. *Journal of Medical Genetics*, 43(4), 306–314. <https://doi.org/10.1136/jmg.2005.036061>
- Kosho, T., Miyake, N., & Carey, J. C. (2014). Coffin-Siris syndrome and related disorders involving components of the BAF (mSWI/SNF) complex: Historical review and recent advances using next generation

- sequencing. *American Journal of Medical Genetics. Part C, Seminars in Medical Genetics*, 166C(3), 241–251. <https://doi.org/10.1002/ajmg.c.31415>
- Lackey, A. E., & Muzio, M. R. (2021). *StatPearls*. StatPearls Publishing.
- Lalani, S. R., Safiullah, A. M., Fernbach, S. D., Harutyunyan, K. G., Thaller, C., Peterson, L. E., McPherson, J. D., Gibbs, R. A., White, L. D., Hefner, M., Davenport, S. L., Graham, J. M., Bacino, C. A., Glass, N. L., Towbin, J. A., Craigen, W. J., Neish, S. R., Lin, A. E., & Belmont, J. W. (2006). Spectrum of CHD7 mutations in 110 individuals with CHARGE syndrome and genotype-phenotype correlation. *American Journal of Human Genetics*, 78(2), 303–314. <https://doi.org/10.1086/500273>
- Landrum, M. J., Lee, J. M., Benson, M., Brown, G. R., Chao, C., Chitipiralla, S., Gu, B., Hart, J., Hoffman, D., Jang, W., Karapetyan, K., Katz, K., Liu, C., Maddipatla, Z., Malheiro, A., McDaniel, K., Ovetsky, M., Riley, G., Zhou, G., ... Maglott, D. R. (2018). ClinVar: Improving access to variant interpretations and supporting evidence. *Nucleic Acids Research*, 46(D1), D1062–D1067. <https://doi.org/10.1093/nar/gkx1153>
- Li, H. (2013). Aligning sequence reads, clone sequences and assembly contigs with BWA-MEM. *arXiv: Genomics*. <https://doi.org/10.48550/arXiv.1303.3997>
- Liu, L., Bu, H., Yang, Y., Tan, Z., Zhang, F., Hu, S., & Zhao, T. (2017). A targeted, next-generation genetic sequencing study on tetralogy of Fallot, combined with cleft lip and palate. *The Journal of Craniofacial Surgery*, 28(4), e351–e355. <https://doi.org/10.1097/SCS.0000000000003598>
- Liu, X., Wu, C., Li, C., & Boerwinkle, E. (2016). dbNSFP v3.0: A one-stop database of functional predictions and annotations for human non-synonymous and splice-site SNVs. *Human Mutation*, 37(3), 235–241. <https://doi.org/10.1002/humu.22932>
- Loenarz, C., Ge, W., Coleman, M. L., Rose, N. R., Cooper, C. D. O., Klose, R. J., Ratcliffe, P. J., & Schofield, C. J. (2010). PHF8, a gene associated with cleft lip/palate and mental retardation, encodes for an Nepsilon-dimethyl lysine demethylase. *Human Molecular Genetics*, 19(2), 217–222. <https://doi.org/10.1093/hmg/ddp480>
- Loomes, K. M., Underkoffler, L. A., Morabito, J., Gottlieb, S., Piccoli, D. A., Spinner, N. B., Scott Baldwin, H., & Oakey, R. J. (1999). The expression of Jagged1 in the developing mammalian heart correlates with cardiovascular disease in Alagille syndrome. *Human Molecular Genetics*, 8(13), 2443–2449. <https://doi.org/10.1093/hmg/8.13.2443>
- Mossey, P. A., & Catilla, E. E. (2001). *Global registry and database on craniofacial anomalies: Report of a WHO Registry Meeting on Craniofacial Anomalies*. World Health Organization.
- Mossey, P. A., & Modell, B. (2012). Epidemiology of oral clefts 2012: An international perspective. *Frontiers of Oral Biology*, 16, 1–18. <https://doi.org/10.1159/000337464>
- Munabi, N. C. O., Swanson, J., Auslander, A., Sanchez-Lara, P. A., Davidson Ward, S. L., & Magee, W. P., 3rd. (2017). The prevalence of congenital heart disease in nonsyndromic cleft lip and/or palate: A systematic review of the literature. *Annals of Plastic Surgery*, 79(2), 214–220. <https://doi.org/10.1097/SAP.0000000000001069>
- Qian, Y., Xiao, D., Guo, X., Chen, H., Hao, L., Ma, X., Huang, G., Ma, D., & Wang, H. (2017). Hypomethylation and decreased expression of BRG1 in the myocardium of patients with congenital heart disease. *Birth Defects Research*, 109(15), 1183–1195. <https://doi.org/10.1002/bdr2.1053>
- Rubinato, E., Rondeau, S., Giuliano, F., Kossorotoff, M., Parodi, M., Gherbi, S., Steffan, J., Jonard, L., & Marlin, S. (2020). MED12 missense mutation in a three-generation family. Clinical characterization of MED12-related disorders and literature review. *European Journal of Medical Genetics*, 63(3), 103768. <https://doi.org/10.1016/j.ejmg.2019.103768>
- Schleiffarth, J. R., Person, A. D., Martinsen, B. J., Sukovich, D. J., Neumann, A., Baker, C. V., Lohr, J. L., Cornfield, D. N., Ekker, S. C., & Petryk, A. (2007). Wnt5a is required for cardiac outflow tract septation in mice. *Pediatric Research*, 61(4), 386–391. <https://doi.org/10.1203/pdr.0b013e3180323810>
- Schwenty-Lara, J., Nehl, D., & Borchers, A. (2020). The histone methyltransferase KMT2D, mutated in kabuki syndrome patients, is required for neural crest cell formation and migration. *Human Molecular Genetics*, 29(2), 305–319. <https://doi.org/10.1093/hmg/ddz284>
- Sevim Bayrak, C., Zhang, P., Tristani-Firouzi, M., Gelb, B. D., & Itan, Y. (2020). De novo variants in exomes of congenital heart disease patients identify risk genes and pathways. *Genome Medicine*, 12(1), 9. <https://doi.org/10.1186/s13073-019-0709-8>
- Shapiro, M. D., & Fazio, S. (2017). Apolipoprotein B-containing lipoproteins and atherosclerotic cardiovascular disease. *F1000Res*, 6, 134. <https://doi.org/10.12688/f1000research.9845.1>
- Sinha, T., Wang, B., Evans, S., Wynshaw-Boris, A., & Wang, J. (2012). Disheveled mediated planar cell polarity signaling is required in the second heart field lineage for outflow tract morphogenesis. *Developmental Biology*, 370(1), 135–144. <https://doi.org/10.1016/j.ydbio.2012.07.023>
- Smedts, H. P., van Uiter, E. M., Valkenburg, O., Laven, J. S., Eijkemans, M. J., Lindemans, J., Steegers, E. A., & Steegers-Theunissen, R. P. (2012). A derangement of the maternal lipid profile is associated with an elevated risk of congenital heart disease in the offspring. *Nutrition, Metabolism, and Cardiovascular Diseases*, 22(6), 477–485. <https://doi.org/10.1016/j.numecd.2010.07.016>
- Toubat, O., Mallios, D. N., Munabi, N. C. O., Magee, W. P., 3rd, Starnes, V. A., & Kumar, S. R. (2021). Clinical importance of concomitant cleft lip/palate in the surgical management of patients with congenital heart disease. *World Journal for Pediatric and Congenital Heart Surgery*, 12(1), 35–42. <https://doi.org/10.1177/2150135120954814>
- Trapnell, C., Williams, B. A., Pertea, G., Mortazavi, A., Kwan, G., van Baren, M. J., Salzberg, S. L., Wold, B. J., & Pachter, L. (2010). Transcript assembly and quantification by RNA-Seq reveals unannotated transcripts and isoform switching during cell differentiation. *Nature Biotechnology*, 28(5), 511–515. <https://doi.org/10.1038/nbt.1621>
- Tsurusaki, Y., Okamoto, N., Ohashi, H., Mizuno, S., Matsumoto, N., Makita, Y., Fukuda, M., Isidor, B., Perrier, J., Aggarwal, S., Dalal, A. B., Al-Kindy, A., Liebelt, J., Mowat, D., Nakashima, M., Saito, H., Miyake, N., & Matsumoto, N. (2014). Coffin-Siris syndrome is a SWI/SNF complex disorder. *Clinical Genetics*, 85(6), 548–554. <https://doi.org/10.1111/cge.12225>
- U.S. National Library of Medicine. (2020a, July 1). MED12 gene: Mediator complex subunit 12. Retrieved from <https://medlineplus.gov/genetics/gene/med12/>.
- U.S. National Library of Medicine. (2020b, July 1). SMARCA4 gene: SWI/SNF related, matrix associated, actin dependent regulator of chromatin, subfamily a, member 4. Retrieved from <https://medlineplus.gov/genetics/gene/smarca4/#conditions>.
- van Buggenhout, G., & Fryns, J. P. (2006). Lujan-Fryns syndrome (mental retardation, X-linked, marfanoid body habitus). *Orphanet Journal of Rare Diseases*, 1, 26. <https://doi.org/10.1186/1750-1172-1-26>
- van de Putte, R., van Rooij, I., Marcelis, C. L. M., Guo, M., Brunner, H. G., Addor, M. C., Caverro-Carbonell, C., Dias, C. M., Draper, E. S., Etxebarriarteun, L., Gatt, M., Haeusler, M., Khoshnood, B., Klungsoyr, K., Kurinczuk, J. J., Lanzoni, M., Latos-Bielenska, A., Luyt, K., ... Bergman, J. E. H. (2020). Spectrum of congenital anomalies among VACTERL cases: A EUROCAT population-based study. *Pediatric Research*, 87(3), 541–549. <https://doi.org/10.1038/s41390-019-0561-y>
- van Ravenswaaij-Arts, C. M., Hefner, M., Blake, K., & Martin, D. M. (1993). CHD7 Disorder. In M. P. Adam, H. H. Ardinger, R. A. Pagon, S. E. Wallace, L. J. H. Bean, G. Mirzaa, & A. Amemiya (Eds.), *GeneReviews*®. University of Washington.
- Verloes, A. (2005). Updated diagnostic criteria for CHARGE syndrome: A proposal. *American Journal of Medical Genetics. Part A*, 133A(3), 306–308. <https://doi.org/10.1002/ajmg.a.30559>

- Warejko, J. K., Schueler, M., Vivante, A., Tan, W., Daga, A., Lawson, J. A., Braun, D. A., Shril, S., Amann, K., Somers, M. J. G., Rodig, N. M., Baum, M. A., Daouk, G., Traum, A. Z., Kim, H. B., Vakili, K., Porras, D., Lock, J., Rivkin, M. J., ... Hildebrandt, F. (2018). Whole exome sequencing reveals a monogenic cause of disease in 43% of 35 families with Midaortic syndrome. *Hypertension*, 71(4), 691–699. <https://doi.org/10.1161/HYPERTENSION.AHA.117.10296>
- Zaidi, S., Choi, M., Wakimoto, H., Ma, L., Jiang, J., Overton, J. D., Romano-Adesman, A., Bjornson, R. D., Breitbart, R. E., Brown, K. K., Carriero, N. J., Cheung, Y. H., Deanfield, J., DePalma, S., Fakhro, K. A., Glessner, J., Hakonarson, H., Italia, M. J., Kaltman, J. R., ... Lifton, R. P. (2013). De novo mutations in histone-modifying genes in congenital heart disease. *Nature*, 498(7453), 220–223. <https://doi.org/10.1038/nature12141>

SUPPORTING INFORMATION

Additional supporting information may be found in the online version of the article at the publisher's website.

How to cite this article: Munabi, N. C. O., Mikhail, S., Toubat, O., Webb, M., Auslander, A., Sanchez-Lara, P. A., Manojlovic, Z., Schmidt, R. J., Craig, D., Magee, W. P. III, & Kumar, S. R. (2022). High prevalence of deleterious mutations in concomitant nonsyndromic cleft and outflow tract heart defects. *American Journal of Medical Genetics Part A*, 188A: 2082–2095. <https://doi.org/10.1002/ajmg.a.62748>